JOURNAL OF MATERIALS SCIENCE 27 (1992) 1212–1216

Microstructure and properties of supersaturated ZA27 alloy during natural ageing

WANG HONGMIN, CHEN QUANDE, WU YIGUI, ZHANG YUANGENG
Department of Materials Engineering, Luoyang Institute of Technology, Henan Province 471039, People's Republic of China

The decomposition of the supersaturated solid solution of ZA27 alloy at room temperature has been investigated by X-ray diffraction, TEM and mechanical properties testing. Based on the results obtained, both continuous precipitation and cellular reaction occur during the decomposition process. The continuous precipitation follows the sequence: $\alpha' \rightarrow \alpha'_1$ + spherical GP zones $\rightarrow \alpha'_2$ + elliptical GP zones $\rightarrow \alpha'_3 + R \rightarrow \alpha + \eta$. The cellular reaction can be written: $\alpha' \rightarrow \alpha + \eta + \varepsilon$. The properties of the alloy depend on the microstructure. After 1 month of ageing, a series of changes of microstructure have taken place. The properties of the alloy are: $\sigma_b = 500$ MPa, $\delta = 13\%$, $H_V = 148$.

1. Introduction

During the last decade, Zn-based alloys have been well developed and increasingly introduced to commercial applications [1]. Some workers have studied the effects of many technologies on the ZA27 alloy [2–4]. The ageing process of as-cast ZA27 alloy has also been studied [5], but the ageing process of supersaturated ZA27 alloy is hardly studied.

Since 1943, in which Guinier observed Guinier–Preston (GP) zones by small-angle X-ray diffraction (XRD) [6], the ageing process of supersaturated Al–Zn alloys has been extensively researched. In 1960, Garward *et al.* [7] found the intermediate phase α' in Al–25% Zn alloy heated to 200 °C by the Debye–Sherrer XRD method. Several years later, another intermediate phase R was detected by Synecek *et al.* [8]. After further testing and verifying, the ageing sequence was written as [9, 10]

$$\alpha'_s \rightarrow \text{GP zones} \rightarrow R \rightarrow \alpha' \rightarrow \eta$$

Moreover, cellular reactions of Al–Zn alloys were studied. It was found that the nucleation of α and η phases occurred first in the grain boundary, then both phases grow up towards the centre of the grains in parallel and alternately. There is a thin diffusion layer around the cellular reaction cell which controls the reaction velocity [11–13].

All the above researches were based on Al–Zn alloys which contained Zn at less than 40 wt %. But what is the sequence in other alloys which contain Zn at more than 70 wt %, such as ZA27 (Zn–27% Al–2% Cu–0.01% Mg)? How do the properties change during the ageing? Both problems are dealt with in this paper.

2. Experimental procedure

2.1. Preparation of alloy

The alloy (Zn–27% Al–2% Cu–0.01% Mg) was prepared using commercial-purity Zn (99.99%), Al (99.7%), Cu (99.90%) and Mg (99.85%) in an electrical furnace. Without degassing and modifying, the melt was poured into a preheated Y-shaped steel mould at 580 °C.

2.2. Heat treatment of the alloy

After homogenizing at 360 °C for 48 h, the samples were quenched. Then they were examined by TEM (H800) and in an X-ray diffractometer (Rigaku 2).

3. Results and discussion

Since the ZA27 alloy is heated to a temperature of about 360 °C, all Zn and Cu atoms are in solid solution as a stable f.c.c. α' phase, and by quenching the specimen there is no time for any transformation to occur so that the solid solution is kept unchanged to room temperature. However, there is a driving force for precipitation of the equilibrium η and ε-$CuZn_4$ phases. During ageing, both continuous and cellular precipitations occur.

3.1. Continuous precipitation

When the supersaturated specimen is aged at room temperature, spherical Zn-rich GP zones precipitate in a very short time. After 1 h ageing, the GP zones grow to about 9 nm in diameter (Fig. 1). It is well known that the atomic radii of Al, Zn and Cu are 0.143, 0.137 and 0.128 nm, respectively. Dissolving of Zn and Cu in Al must cause negative deformation, so the distances between crystal planes of α' will become smaller than those of Al. The varying trend (θ) can be obtained from the equation

$$\theta(\%) = 100 \frac{d_{Al} - d_{\alpha'}}{d_{Al}}$$

0022–2461

According to this equation and the $d_{\alpha'}$ values obtained by XRD, the varying trends of crystal planes in α' are shown in Table I.

It is shown in Table I that the θ of $(1\,1\,1)_{\alpha'}$ is the biggest. This means that concentration of Zn and Cu in $(1\,1\,1)_{\alpha'}$ is the maximum. This makes the GP zones turn into elliptical GP zones (Fig. 2). After 80 min, the long and short axes of elliptical GP zones are 23 and 12 nm, respectively, with the long axis parallel to $(1\,1\,1)_{\alpha'}$.

Comparing the diffraction pattern in Fig. 1 with that in Fig. 2, it is seen that the diffusion of diffraction spots becomes greater in Fig. 2, which suggests that coherent strain caused by GP zones is more serious as the GP zones grow. This result can be explained by the GP zones being bigger in size and richer in concentration. When the coherent strain reaches a certain range which the matrix cannot bear, the coherent relations between GP zones and matrix will be partly destroyed; a semi-coherent relation builds up and the intermediate phase R forms at the same time.

After 100 min the intermediate phase R forms. This result can be observed in the diffraction pattern. According to Carpenter's research [9] on Al–22% Zn alloy, the structure of phase R is a face-centred

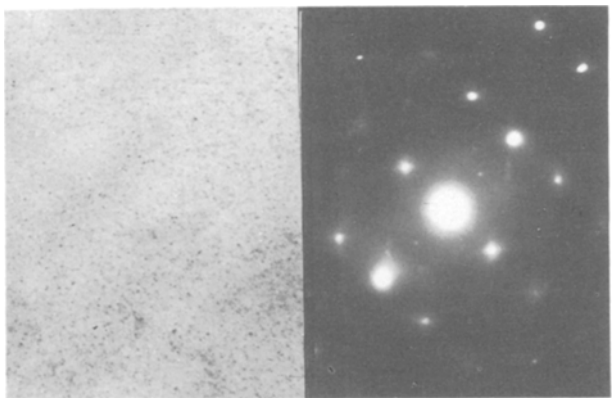

Figure 1 α' + GP zones (spherical). (× 40 000)

TABLE I The varying trends of crystal planes in α'

Planes	(1 1 1)	(2 0 0)	(2 2 0)	(3 1 1)	(2 2 2)
θ (%)	2.18	1.93	1.68	1.56	1.54

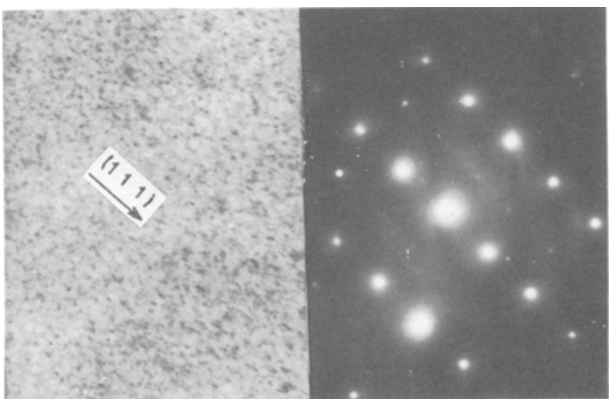

Figure 2 α' + GP zones (elliptical). (× 40 000)

rhombohedron, $a = 0.4005$ nm. However, in ZA27, $a = 0.3847$–0.3965 nm as determined by XRD. We think the varying of a exactly proves that phase R is a growing, non-equilibrium phase. Perhaps the higher concentration of zinc leads to the smaller a of phase R than Carpenter's.

In addition, we find that phase R nucleates in GP zones, so that GP zones have provided nucleation sites. As GP zones grow, the Zn atoms in GP zones enrich more and more, and the coherent strain becomes stronger and stronger. At last, the coherent relation is partly damaged and the matrix brings pressure to bear on the GP zones. This makes the GP zones become R phase which is semi-coherent with the matrix. In this process we can imagine that the lattice constants of the R phase depend on the concentration and size of the R phase, so it can be deduced that the crystal structure and orientation of the R phase are similar to those of the matrix.

As the R phases grow, more serious strain in the R–α' interfaces is developed, and a richer Zn concentration is gained. The new phase η nucleates in the R–α' interfaces and grows by swallowing R phases, i.e. R–α' interfaces provide sites for η nucleation, and R is the food for η growth. Based on the relationship between R and α', most η-phase particles exist in the matrix with $(1\,1\,1)_{\alpha'} \| (1\,0\cdot 1)_{\eta}$.

The continuous precipitation can therefore be summed up as follows:

$$\alpha' \rightarrow \alpha'_1 + \text{GP (spherical)} \rightarrow \alpha'_2 + \text{GP (elliptical)}$$
$$\rightarrow \alpha'_3 + \text{R} \rightarrow \alpha + \eta$$

All the micrographs were taken in the same sample. Because of the electronic beam action and the higher temperature, the precipitation process in TEM is faster than at room temperature.

3.2. Cellular reaction

After about 120 h natural ageing, cellular reaction will take place in supersaturated ZA27 alloy. In contrast with other alloys, there are three characteristics in the ageing process of the supersaturated ZA27 alloy:

(i) Not only the grain boundary but also the inside of a grain can nucleate for cellular reaction. This is because there are enormous quantities of η phase in a grain and most of these η phases are in the same orientation. When an η-phase particle grows up to a certain dimension, it will connect with adjacent η phases and become a big particle; both particles of phase η and the adjacent phase α as a cell nucleus grow into the surrounding grains (Fig. 3). Instead of a single α', three phases (R, η, α') are in the front of the cellular reaction cell; the cell development does not depend on a cell boundary diffusion layer, but on the merging of α and η phases. This makes α and η in a cell bend and branch (Fig. 4).

(ii) The cellular reaction can be written as follows:

$$\alpha' \rightarrow \alpha + \eta + \varepsilon$$

where the ε phase contains compounds of $CuZn_4$. When α and η grow, Cu atoms are pushed out to η–α'

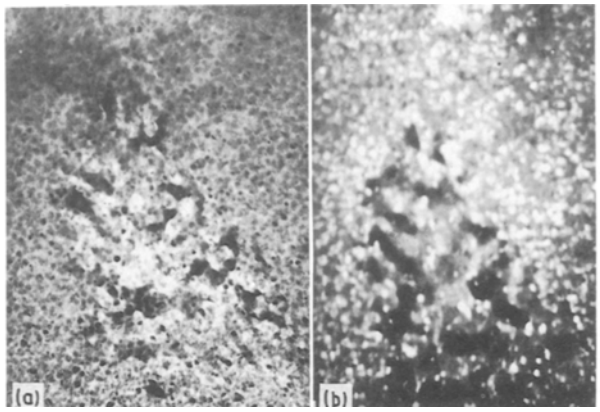

Figure 3 Cellular reaction beginning inside the α′ phase: (a) bright field, (b) dark field. (× 50 000)

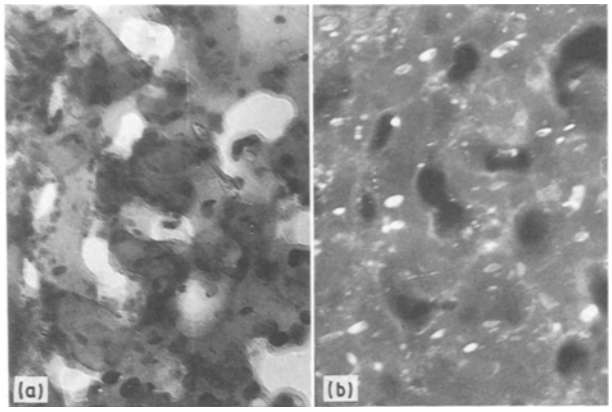

Figure 5 Nucleation and growth of $CuZn_4$: (a) bright field, (b) dark field. (× 10 000)

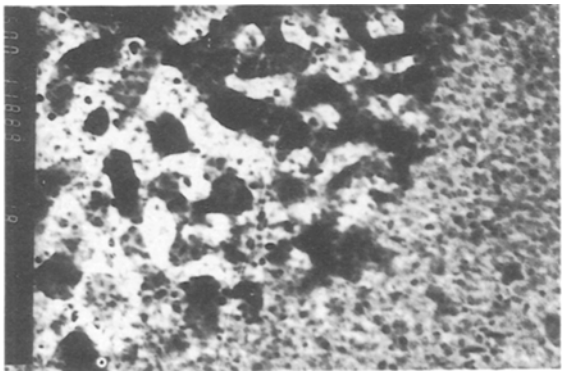

Figure 4 Cellular reaction area. (× 60 000)

and α–α′ interfaces and develop a Cu-rich layer. As the Cu atoms are further enriched in the layer, $CuZn_4$ compounds nucleate and coarsen. These facts are demonstrated in Fig. 5, which shows the Cu-rich layer and coarse $CuZn_4$ particles.

(iii) The cellular reaction consists of two parts. In the first, the α and η phases connect with each other in the cell boundary, making the cell larger and larger. In the second, every phase in the cell precipitates further and forms equilibrium phases. In Fig. 3 there are R phases in the cell which are going to transform to η. In this way, the cellular reaction can be written as

$$\alpha' + R + \eta \rightarrow \alpha + \eta + \varepsilon$$

In brief, the cellular reaction is the process of phases precipitating further and merging with each other. As the alloy ages, the branching grains in a cell coarsen and reach polygonal equilibrium grain size.

3.3. The effect of microstructures on the mechanical properties

To further prove these conclusions, we have studied the ageing process of supersaturated ZA27 alloy with XRD (Fig. 6). In the initial stage of the ageing, α′-phase diffraction peaks move to the left. This means that the lattice constants of the α′ phase become larger. In the middle and last stages, the peaks of α′ grow weaker and weaker, while the peaks of α, η and ε phases grow stronger and stronger. So, continuous and cellular reactions are proved by XRD as well.

We also tested the mechanical properties (Fig. 7) to study the effect of phases on the mechanical properties. In addition, the trends of the quantity change of every phase are illustrated according to the peak intensity of every phase in Fig. 8. The following effects are demonstrated clearly in the two figures:

(i) *Initial stage.* In this early period, the microstructure of the aged alloy is α′ + GP zones + R, and the R phase is increasing more and more. Both hardness and tensile strength increase and the elongation decreases. This is because of the good deformation ability of α′ and the small dislocation moving resistance of GP zones. Phase R has a somewhat stronger resistance to the movement of dislocations, but there are too few R-phase particles in the microstructure, so the alloy shows lower H_V and σ_b and a higher δ. The more the R phase develops, the stronger is the dislocation movement resistance. When the R phase precipitates everywhere in the α′ phase in very tiny particles, dislocations will be locked between R-phase particles. The alloy now displays higher σ_b and H_V and a lower δ.

(ii) *Middle stage.* α′ and R phases decrease and α, η and ε phases increase gradually. This makes H_V and σ_b decrease and δ increase. As the R phase transforms to η phase and cellular reaction proceeds, the R phase gets less and the dislocation moving resistance gets weaker too. Meanwhile, because the precipitation is progressing, the α′ phase possesses a lower excess of solute and solid-solution strengthening will be weaker. Thus H_V and σ_b of the alloy decrease and δ increases.

(iii) *Last stage.* α′ and R-phase in the microstructure decrease and disappear, while α, η and ε phases increase and tend to become stable. H_V, σ_b and δ increase and become stable too. As cellular reaction proceeds, the ε phase increases and disperses in tiny particles. If a dislocation moves through an ε-phase, antiphase domain-boundary energy and additional surface energy will arise so that σ_b and H_V rise. However, the quantity of ε-phase is much less than for the earlier R phase, so there are still many places for dislocations to move. In addition, the equilibrium

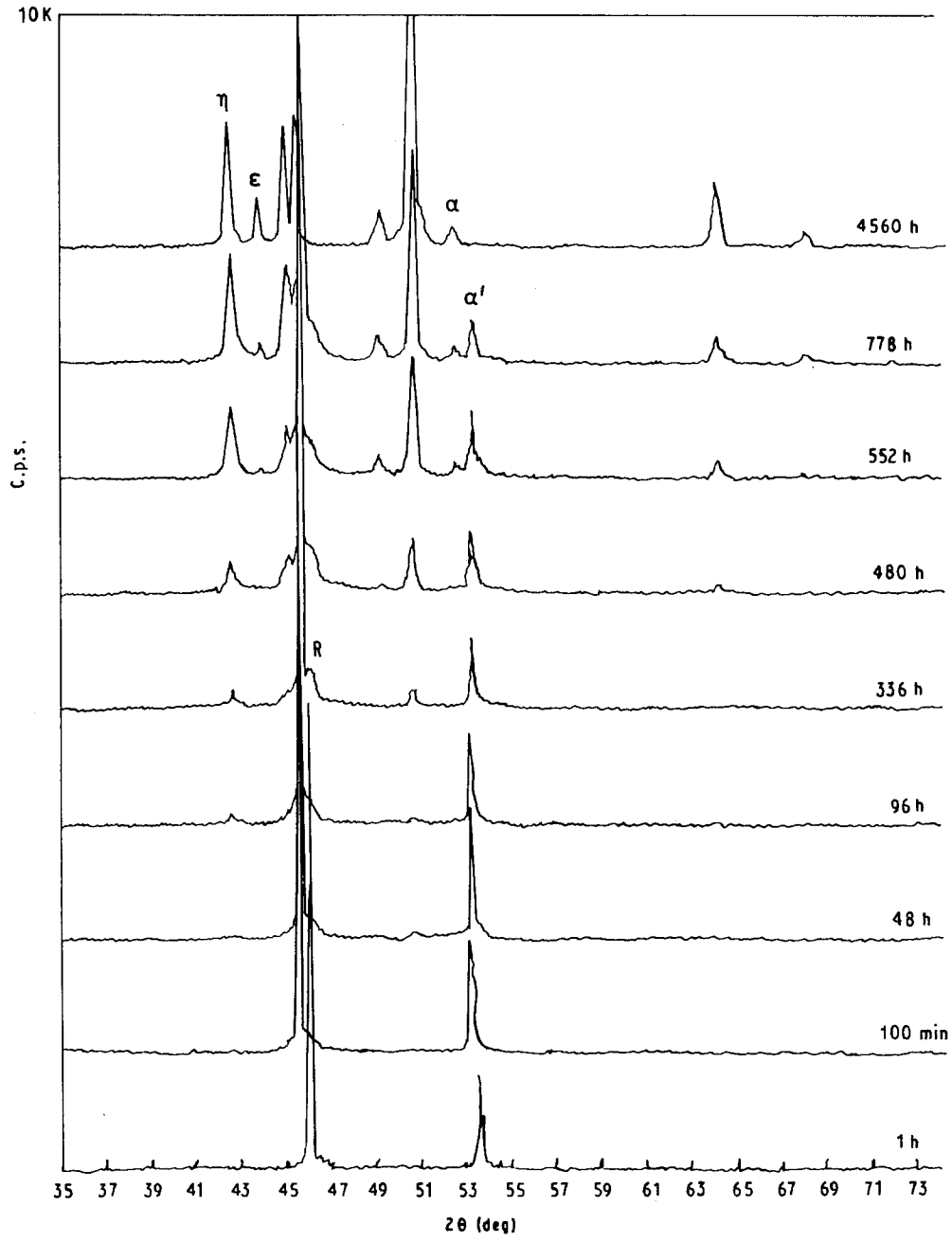

Figure 6 A set of XRD patterns of supersaturated ZA27 during ageing at room temperature.

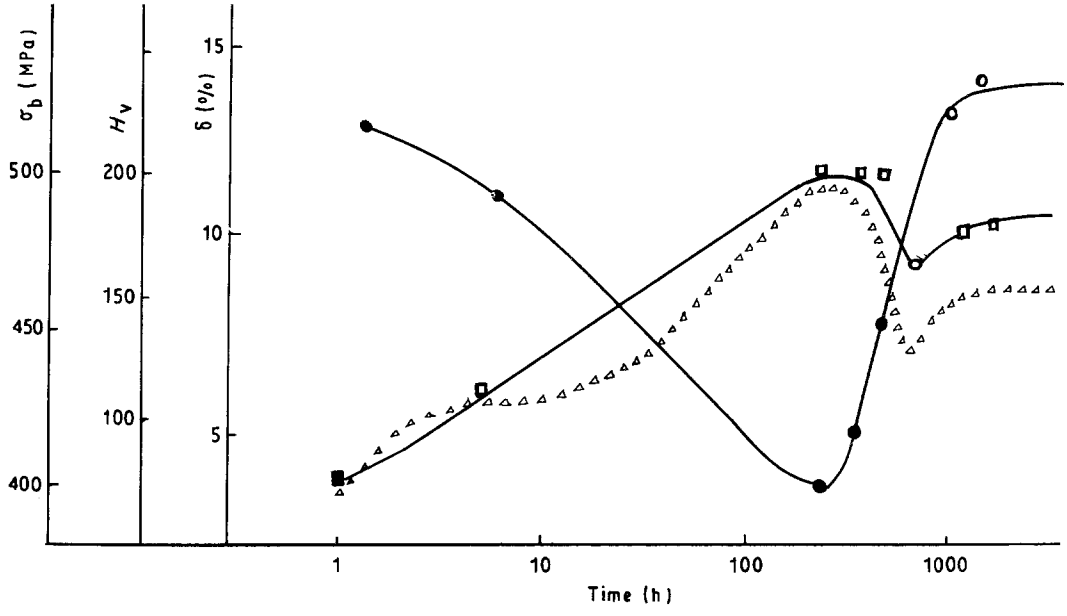

Figure 7 The changing trends of mechanical properties during ageing at room temperature: (△) H_V, (□) σ_b, (○) δ.

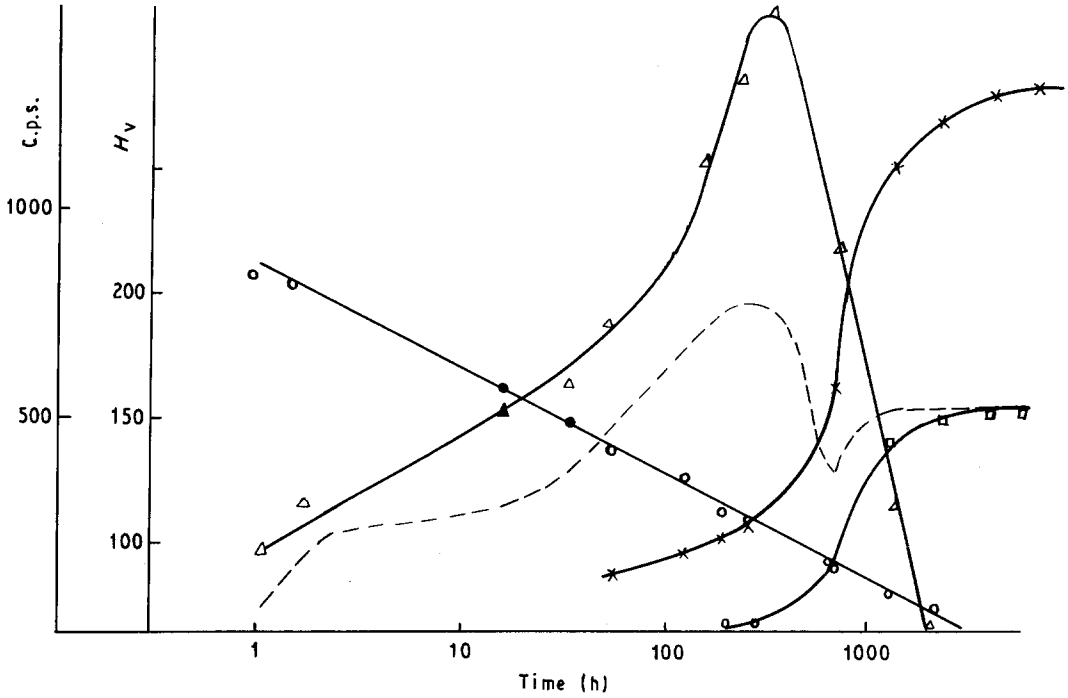

Figure 8 The changing trends of phases during ageing at room temperature. (○) α′ (200), (△) R (111), (×) α (2000), (□) η (10·2), (●) ε (00·2). (——) cps, (– – –) H_v.

α-phase provides dislocations with the best place to move. All this makes the elongation increase. When the crystal grains reach the equilibrium grain dimension at room temperature, the phase transformation ends and the mechanical properties become stable.

4. Conclusions

1. For supersaturated ZA27 alloy ageing at room temperature, phase transformation will begin with continuous precipitation. The sequence is

$$\alpha' \rightarrow \alpha'_1 + \text{GP zones (spherical)}$$
$$\rightarrow \alpha'_2 + \text{GP zones (elliptical)}$$
$$\rightarrow \alpha'_3 + \text{R} \rightarrow \alpha + \eta$$

In the middle and last stages, cellular reaction will occur:

$$\alpha' \rightarrow \alpha + \eta + \varepsilon$$

2. For ZA27 alloy, 360 °C/48 h + quenching + natural ageing is an effective heat-treatment technology. After about one month of ageing at 8–18 °C, the σ_b, δ and H_V of the alloy will be 500 MPa, 13% and 148, respectively.

References

1. E. GERVAIS, H. LEVERT and M. BESS, *AFS Trans.* **88** (1980) 183.
2. H. LEHEY, in Proceedings of 25th Annual Conference of Metallurgists, 17–20 August 1986, Toronto, Ontario, pp. 143–153.
3. B. LESLIE and B. BUNCH, *ibid*, pp. 265–274
4. MICHIHIRO TAGAMI and HITOSHI OIKAWA, *Light Metals* **33** (1983) 9.
5. Y. H. ZHU, in Proceedings of 25th Annual Conference of Metallurgists, 17–20 August 1986, Toronto, Ontario, pp. 25–33.
6. A. GUINIER, *Metaux Corros. Usure* **18** (1943) 209.
7. R. D. GARWOOD and A. D. HOPKIN, *J. Inst. Met.* **88** (1959–60) 375.
8. V. SYNECEK *et al.*, in Proceedings of Annual Pittsburgh Diffraction Conference, 4–6 October 1964, p. 30.
9. G. J. C. CARPENTER, *Met. Sci. J.* **1** (1967) 202.
10. M. SIMERSKA, *Acta Metall.* **15** (1967) 223.
11. T. R. ANANTHARAMA, *J. Mater. Sci.* **9** (1974) 240.
12. A. PAWLOWKI and W. TRUSZKOWSKI, *Acta Metall.* **30** (1982) 37.
13. PORTER, "Phase Transformation in Metals and Alloys (Van Nostrand-Reinhold, 1981) p. 332.

Received 9 November 1990
and accepted 10 April 1991